Supporting Information

Flexible electrochemical sensor for highly sensitive and selective non-enzymatic detection of creatinine *via* electrodeposited copper over Polymelamine formaldehyde

Daisy Mehta, Alankar Kafle and Tharamani C. Nagaiah*

Experimental Section

Material and apparatus

All chemicals and solvents were of analytical reagent grade and used without any further purification. Paraformaldehyde, Melamine, Potassium ferrocyanide (>99%), $CuCl_2.2H_2O$, KH_2PO_4, K_2HPO_4, KCl, and isopropyl alcohol were purchased from Loba chemie. All the experiments were performed in 0.1 M of PBS buffer of pH 7.4. All the aqueous solutions were prepared by using deionized water obtained from Millipore system with resistivity (>12 MΩ cm^{-1}).

Synthesis of electrocatalyst (eCu-PMF)

Polymelamine formaldehyde (PMF) was synthesized via one-pot synthesis briefly, both the monomers, melamine (0.378 g, 3 mmol) and paraformaldehyde (1.8 eq., 0.162 g, 5.4 mmol) were mixed with 3.36 mL (overall concentration of 2.5 M of dimethyl sulfoxide (DMSO) in a Teflon container protected in a steel reactor. The reaction mixture was heated to 120 °C in an oven for 1 h. The reactor was kept for stirring for 15 minutes to obtain a homogeneous solution. The solution was then heated to 170 °C for 72 h. The reaction was allowed to cool at room temperature, then crushed, filtered, and washed with different solvents DMSO, acetone, tetrahydrofuran (THF) and CH_2Cl_2.The resulting filtered solid was dried in oven 80 °C for 24 h.[1]As obtained product was physically grinded using mortar pestle and homogenous slurry was prepared by dispersing 1.3 mg of composite in 500 µL containing isopropyl alcohol (IPA 100 µL) and Millipore water (400 µL, 12 MΩ) by ultrasonication for 30 min. Afterwards, 20 µL (52 µg) of as prepared slurry was drop casted on graphite electrode and dried at room temperature. Copper nanoparticles were electrochemically deposited over fabricated graphite electrode using constant voltage chronoamperometry by immersing the electrode in $CuCl_2.2H_2O$ (10mML^{-1}) solution at -0.3 V vs. Ag/AgCl for 4 minutes (Fig. S1a).

Physical Characterization

The produced material was assessed using an X-ray diffractometer (XRD). PAN analytical X'Pert-Pro diffraction system with CuKα radiation 1.54064 nm and was operated at 45 kV, 40 mA, and a scanning speed of 2°/min. spanning from 5 to 80°. Morphological examination was carried out using a scanning electron microscope (SEM, JEOL, JSM-6610l) operating at 20 kV. FT-IR spectra were obtained using a BRUKER TENSOR-27 spectrometer in the range of 600-4000 cm^{-1} with a spectral resolution of 4 cm^{-1} and number of scans 100. The specific surface area of the sample was measured by adsorption of liquid nitrogen at 77 K and by applying the Brunauer–Emmett–Teller (BET) calculation. A prominent peak at 2θ equal to 26.6° was designated to graphitic carbon of carbon paper used for electrodeposition of copper over PMF to form eCu-PMF composite.

Electrochemical measurements

All the electrochemical measurements were performed using Bio-logic VSP-300 workstation controlled by EC-Lab V11.12 software. The electrochemical experiments were conducted using a three-electrode assembly consisting of a graphite electrode (2 mm) as the working electrode, Ag/AgCl/3M KCl electrode as the reference electrode, and platinum wire as an auxiliary/counter electrode. Cyclic voltammetry (CV), square wave voltammetry (SWV), and electrochemical impedance spectroscopy (EIS) techniques were used for all of the analysis using a three-electrode assembly in 2 mL of 0.1 M phosphate buffer (pH 7.4) containing 100 mM KCl as the supporting electrolyte, CV measurements were carried out at room temperature between potential ranges of - 0.5 to 0.5 V vs. Ag/AgCl/3M KCl at a scan rate of 25 mV s^{-1}. SWV measurements were done with step potential 10 mV, pulse amplitude 50 mV, pulse width 100 ms and at a scan rate of 25mV s^{-1} between -0.5 V to 0.3 V. The EIS measurements were performed over a frequency range between 700 kHz to 13 μHz.

Electrochemical surface area (ECSA)

The electrochemical surface area (ECSA) was ascertained by calculating the "double-layer pseudo-capacitance" (C_{dl}) in 0.1 M PBS (pH 7.4) containing 100 μM of creatinine. Cyclic voltammetry tests were performed in the non-faradaic region at various scan rates from 75 to 250 mV s^{-1} over a potential range from -0.2 to 0.3 V. Slope obtained from the plot of averaged current (I_a+I_c)/2; ('I_a' denotes anodic current and 'I_c' is for cathodic current) density at a potential -0.04 V *vs.* the scan rate gives C_{dl}. As obtained C_{dl} was dividing with the specific capacitance of the flat standard surface (20-60 μF cm^{-2}) which in the current study is considered to be 40 μF cm^{-2}, gives electrochemical surface area (ECSA). The roughness of the surface was calculated by dividing the obtained ECSA with the geometrical surface area to result in the roughness factor (R_f).

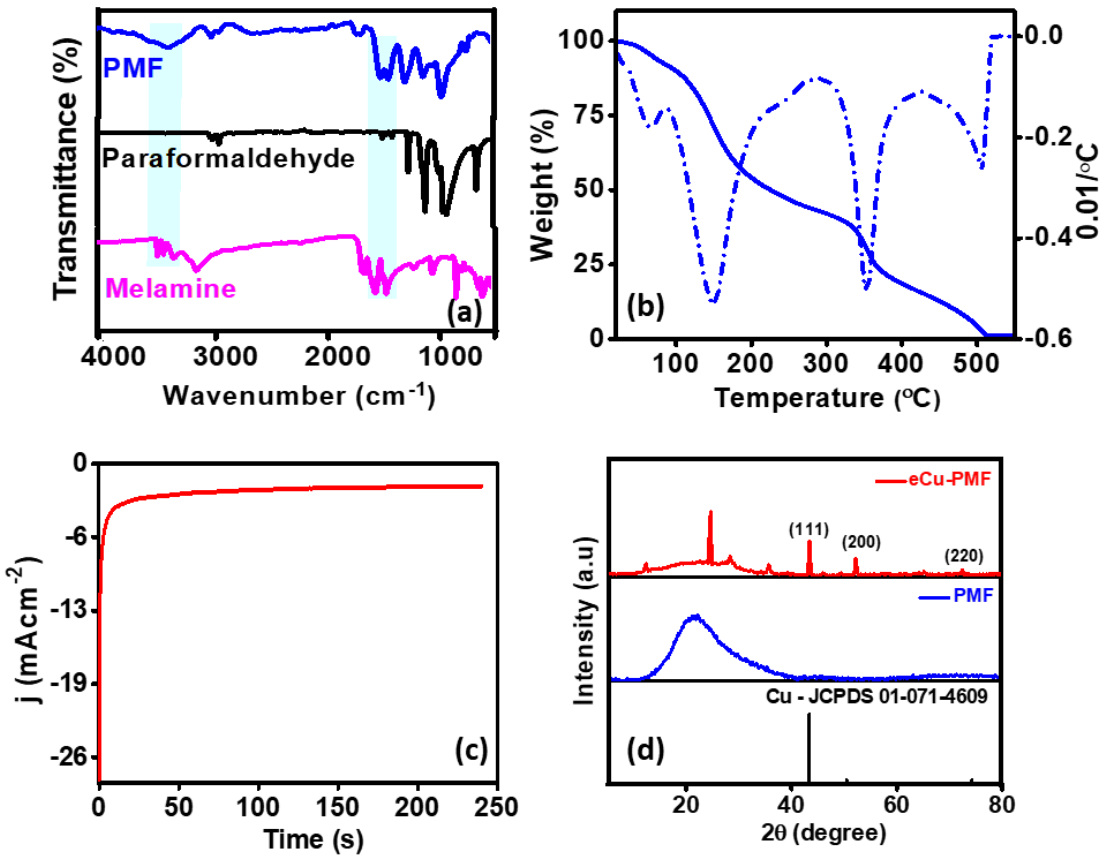

Fig. S1 (a) Comparative FTIR analysis of PMF with respect to melamine and paraformaldehyde (b) TGA curve and 1st derivative showing the weight loss of polymelamineformaldehyde (PMF). (c) Chronoamperometric curve recorded during electrodeposition of copper nanoparticles (d) PXRD pattern of PMF and eCu-PMF.

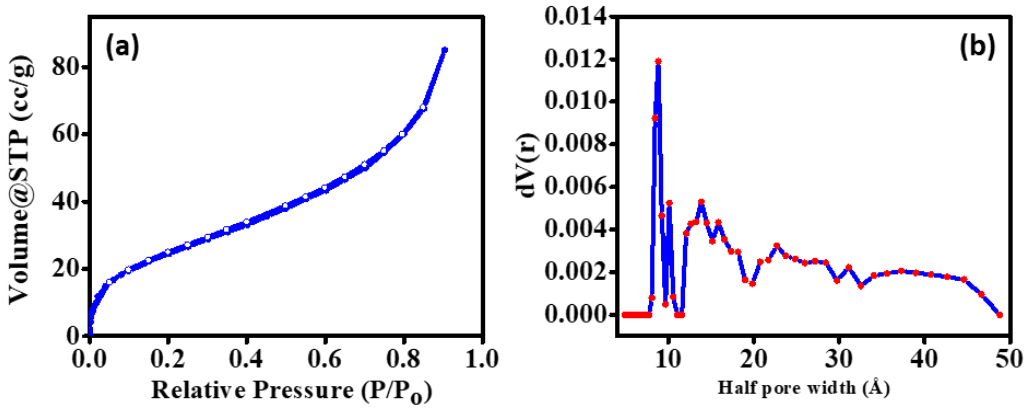

Fig. S2 (a) N2 adsorption/desorption isotherms of PMF (b) Corresponding pore size curve

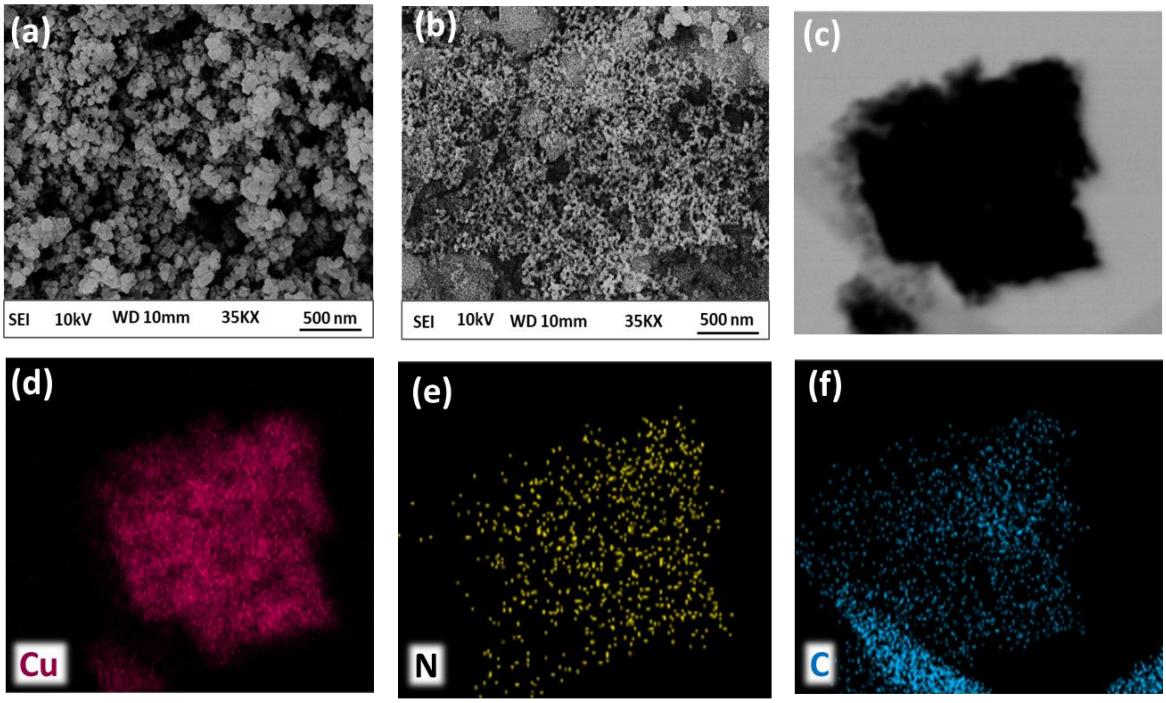

Fig. S3 (a) Fe-SEM image of (a) PMF (b) eCu-PMF (c-f) TEM-EDS dot mapping presenting elemental distribution of various elements (Cu,N and C) in eCu-PMF composite.

Table S1. TEM-EDS compositional analysis of eCu-PMF composite

Element	Wt%
C	10.15
N	15.02
O	3.43
Cu	71.40
Total:	100.00

Table S2. Calculation of charge transfer resistance (R_{ct})

Material	R_{ct} (Ω)	Rate constant (K^0) Mol cm^{-2}
Bare	238	----------
PMF	213	0.805×10^{-3}
eCu-PMF	160	1.07×10^{-3}

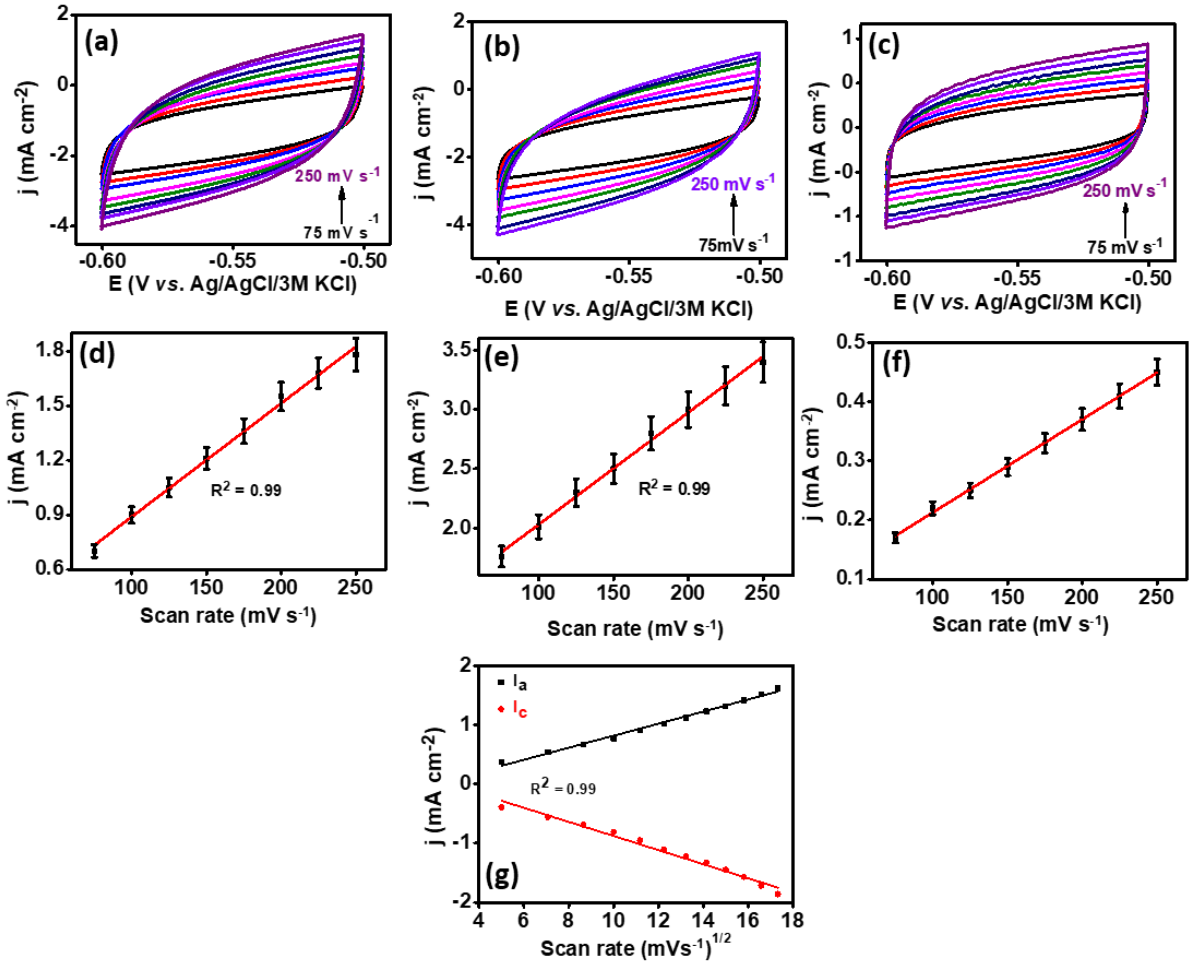

Fig. S4 Cyclic voltammograms of (a) PMF (b) eCu-PMF (c) eCu-PMF in presence of 100 µM of creatinine in non-faradaic region at various scan rates from 75 mVs^{-1} to 275 mVs^{-1} (e)-(f) Corresponding calibration curves for average current density and scan rate. (g) Linearity graph between current density and square root of scan rate extracted from figure 2d.

Table S3. Calculation of electrochemically active surface area

Sample	Catalyst	C_{dl} (µF) at 0.199 V *vs.* Ag/AgCl	ECSA (cm^2)	Surface roughness factor
1.	PMF	9.4	0.23	7.4
2.	eCu-PMF	15.9	0.40	12.9
3.	eCu-PMF/Creatinine	6.24	0.15	4.8

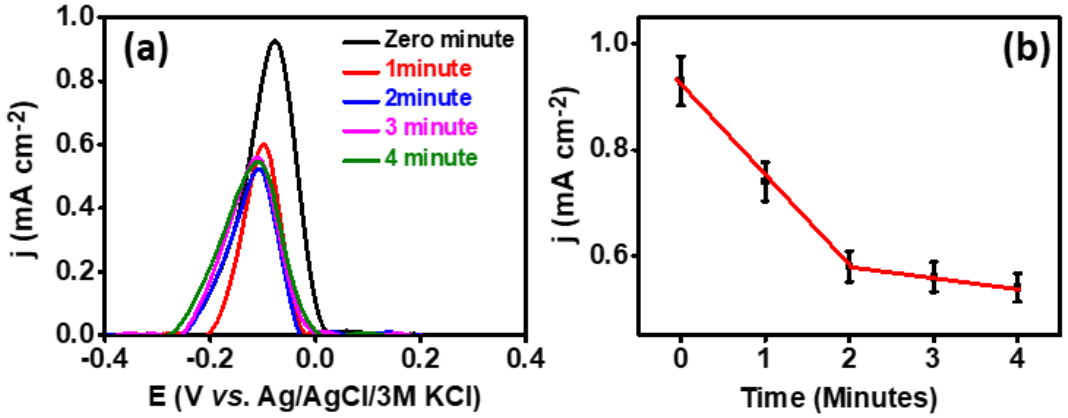

Fig. S5. (a) SWV for Optimization of response time of creatinine (b) corresponding peak current density vs. time curve.

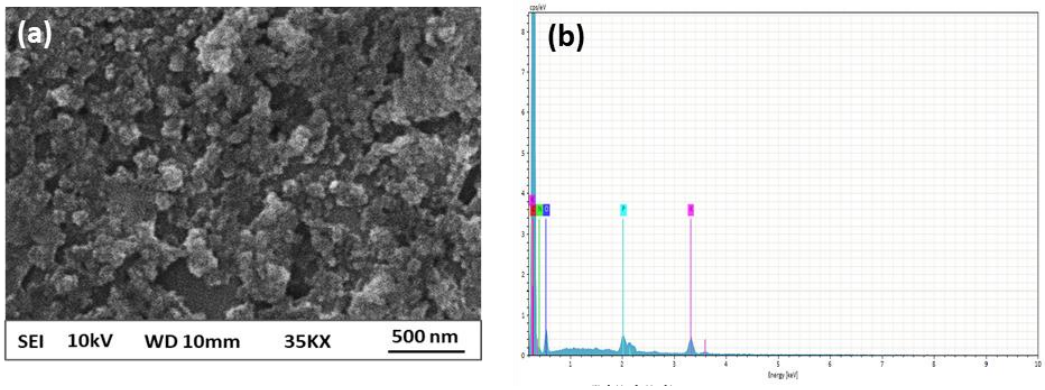

Fig. S6. (a) SEM image and (b) EDS spectra of eCu-PMF modified electrode after concentration studies of creatinine showing the absence of copper over the surface.

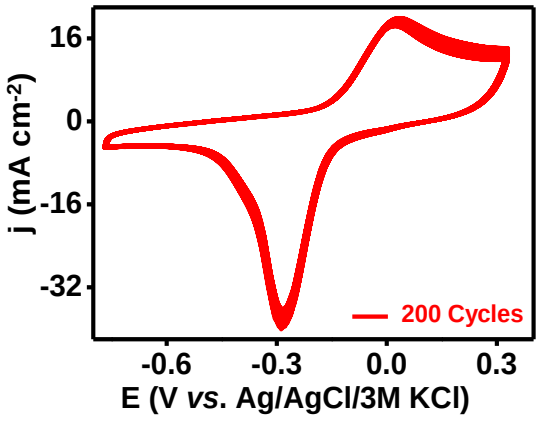

Fig. S7 Cyclic voltammogram of eCu-PMF modified electrode for 200 cycles at scan rate of 25 mV s^{-1}in 0.1M PBS containing 100 µM of creatinine.

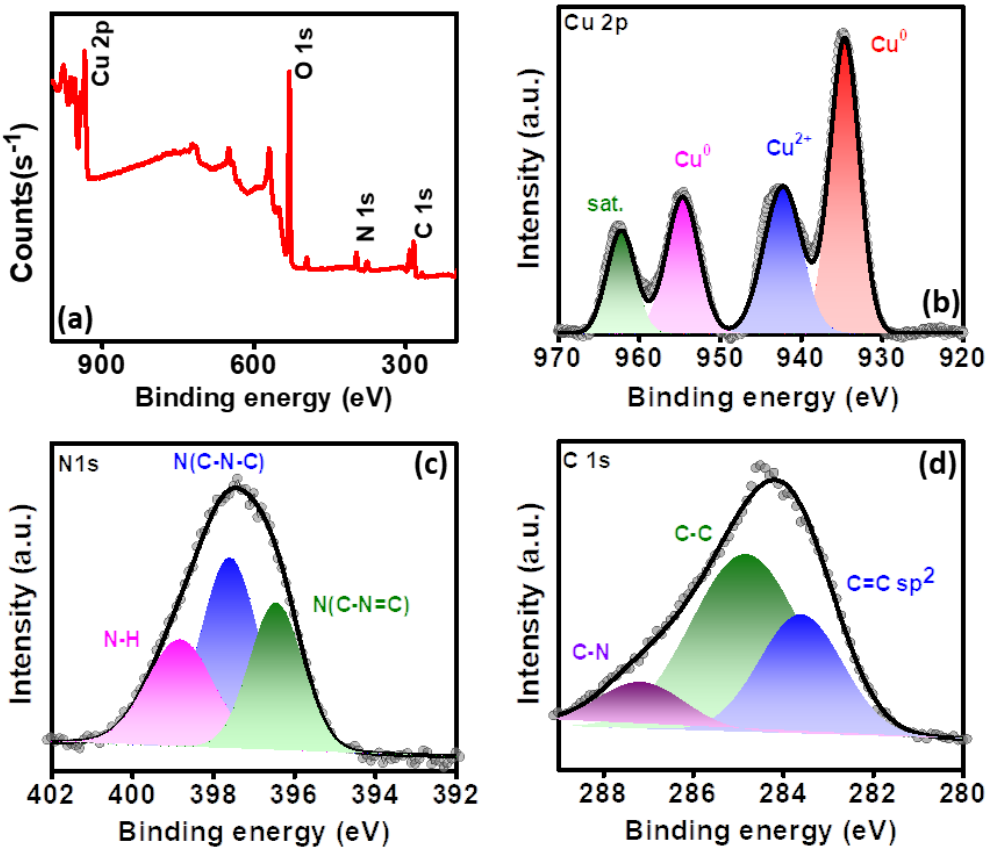

Fig. S8 Post stability analysis (a) XPS survey spectrum and XP deconvoluted (a) Cu 2p (b) N 1s and (c) C 1s of eCu-PMF.

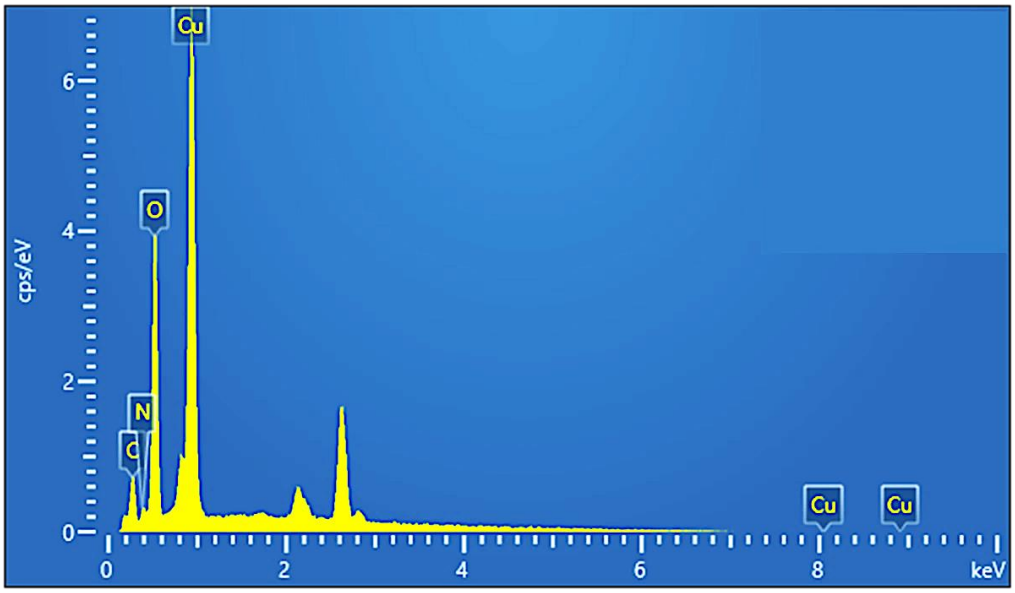

Fig. S9 EDX analysis showing the presence of after 200 CV cycles in the presence of 100µM of creatinine.

Table S4. Comparison of the analytical performance of eCu-PMF modified creatinine sensor with previously reported literatures.

Substrate Material	Detection Range (µM)	Lowest Limit of detection (LOD)	Sensitivity	Ref.
Cu_SPCE	6 - 378	0.0746	----	[2]
PPA-Gel Cu/Cu_2O NP	200 - 100000	6.5	-----	[3]
rGO /Ag NP	0.00001-0.00012	7.43 X 10^{-7}	------	[4]
CNT-ABTS / Nafion	0 - 21300	11	23.7 µA cm^2 mM^{-1}	[5]
Cu/IL/ERGO	10 - 2000	0.22		[6]
CuO/MIP	0.5-200	0.083		[7]
Sb - NPC	0.6 - 1.0	0.74		[8]
CP/MWCNT/Inu	0.2 – 1 & 50 - 12000	0.06, 90	-	[9]
Cu-NP/PDA/rGO/NB	0.01 - 100	0.002		[10]
MIP/Au	0.00088 – 0.0084	0.00014		[11]
Nafion/Polyacrylic gel-Cu/Cu_2O NPs	1-2000	0.3		[12]

MIP-Ni@PANI NPs	0.004 - 0.8	0.0002		[13]
TMSPMA/GO-co/HEMA/MMA	44.2 - 265.2	16.6		[14]
Fe^{3+}- CB / NPs	100 - 6500	43		[15]
Pectin/MWCNT	0.016 – 3.3	0.6241		[16]
CdS Quantum dots	0.442 - 8840	0.229		[17]
CDs / WO_3@GO	0.0002 – 0.112	0.00002		[18]
Mxene - Cu ions	10 - 400	1.2		[19]
PMB-PVAc/Cu/CuNF	0.04 – 7.96	0.02		[20]
CuAg/NP/Nafion	0 - 320	40		[21]
Fe-Cu-rGO	0.01-1000	0.01		[22]
eCu-PMF	$100 \times 10^{-9} – 60 \times 10^{3}$	13.2×10^{-6}	0.320 $mAnM^{-1}cm^{-2}$ & 3.87 $mAnM^{-1}cm^{-2}$	This Work

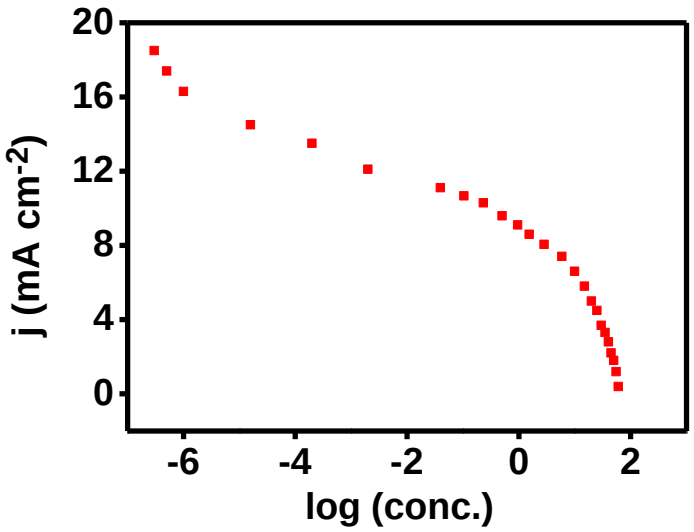

Fig. S10 Logarithmic scale of calibration curve between concentration and peak current density extracted from 2e.

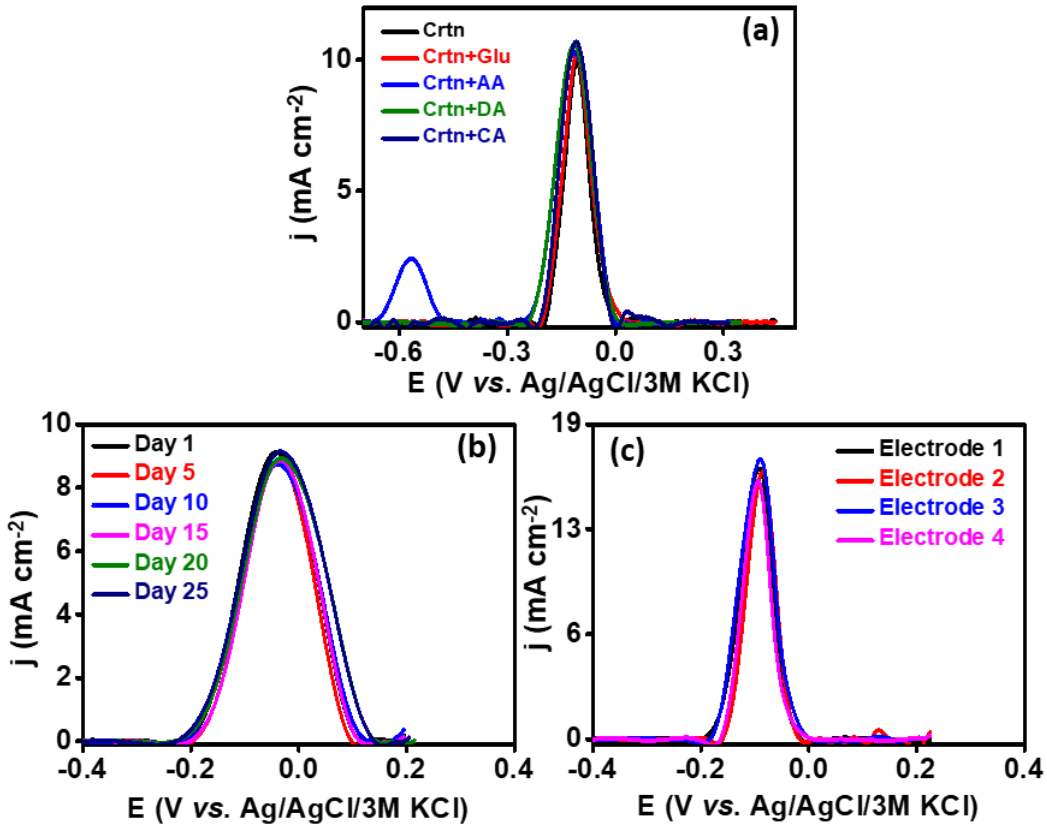

Fig. S11 SWV showing (a) response of different interferents (b) reproducibility of different electrodes. (c) Storage stability.

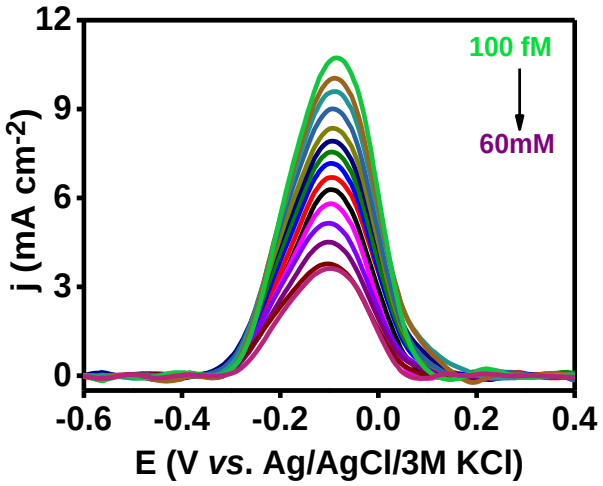

Fig. S12 SWV showing the response of eCu-PMF modified in 0.1M PBS (pH-7.4) at various concentration creatinine in real serum samples.

Table S5. Human serum sample analysis for creatinine				
	Actual conc.(μM)	Conc. Added (μM)	Conc. Found (μM)	Recovery (%)
1.	3.7	20	23	96.5
2	3.7	30	36	107.6
3	3.7	40	49	113
4	3.7	50	61	114

References

1. Raveendran, J.; Resmi, P.; Ramachandran, T.; Nair, B. G.; Babu, T. S., *Actuators B Chem.* 2017, *243*, 589-595.
2. Kalasin, S.; Sangnuang, P.; Khownarumit, P.; Tang, I. M.; Surareungchai, W., *ACS Biomater. Sci. Eng.* 2020, **6** (2), 1247-1258.
3. Viswanath, K. B.; Devasenathipathy, R.; Wang, S. F., *Electroanalysis* 2017, **29** (2), 559-565.
4. Ciou, D.-S.; Wu, P.-H.; Huang, Y.-C.; Yang, M.-C.; Lee, S.-Y.; Lin, C.-Y., *Sens. Actuators B Chem.* 2020, **314**, 128034.
5. Boobphahom, S.; Ruecha, N.; Rodthongkum, N.; Chailapakul, O.; Remcho, V. T., *Anal.Chim. Acta* 2019, **1083**, 110-118.
6. Nontawong, N.; Amatatongchai, M.; Thimoonnee, S.; Laosing, S.; *J. Pharm. Biomed. Anal.* 2019, ***175***, 112770.
7. Jamil, M.; Fatima, B.; Hussain, D.; Chohan, T. A.; Majeed, S.; Imran, M.; Khan, A. A.; Manzoor, S.; Nawaz, R.; *Bioelectrochemistry* 2021, **140**, 107815.
8. Kalaivani, G. J.; Suja, S., *New J. Chem.* 2019, **43** (15), 5914-5924.
9. Gao, X.; Gui, R.; Guo, H.; Wang, Z.; Liu, Q., *Sens.Actuators B.Chem.* 2019, **285**, 201-208.
10. Diouf, A.; Motia, S.; El Hassani, N. E. A.; El Bari, N.; Bouchikhi, B., *J.Electroanal.Chem.* 2017, **788**, 44-53.
11. Kalasin, S.; Sangnuang, P.; Khownarumit, P.; Tang, I. M.; Surareungchai, W.,*ACS Biomater. Sci.Eng.* 2020, **6** (10), 5895-5910.
12. Rao, H.; Lu, Z.; Ge, H.; Liu, X.; Chen, B.; Zou, P.; Wang, X.; He, H.; Zeng, X.; Wang, Y., *Microchim.Acta* 2017, **184** (1), 261-269.
13. Anirudhan, T.; Deepa, J.; Stanly, N., *Appl.surf. sci.* 2019, **466**, 28-39.
14. Fava, E. L.; do Prado, T. M.; Garcia-Filho, A.; Silva, T. A.; Cincotto, F. H.; de Moraes, F. C.; Faria, R. C.; Fatibello-Filho, O., *Talanta* 2020, **207,** 120277.
15. Yazhini, K.; Suja, S.; Bagyalaksmi, J.; Pavalamalar, S.,. *Appl.Surf. Sci.* 2018, **449**, 736-744.

16. Pedrozo-Penafiel, M. J.; Lopes, T.; Gutierrez-Beleno, L. M.; Da Costa, M. E. M.; Larrude, D. G.; Aucelio, R. Q., *J. Electroanal. Chem.* 2020, **878**, 114561.

17. Ponnaiah, S. K.; Prakash, P., *Mater. Sci. Eng. C* 2020, **113**, 111010.

18. Liu, J.; Jiang, X.; Zhang, R.; Zhang, Y.; Wu, L.; Lu, W.; Li, J.; Li, Y.; Zhang, H., *Adv.Funct.Mater.* 2019, **29** (6), 1807326.

19. Pandey, I.; Bairagi, P. K.; Verma, N., *Sens. Actuators B Chem.* 2018, **277**, 562-570.

20. García-Barajas, M.; Trejo-Domínguez, A.; Ledesma-García, J.; Arriaga, L.; Contreras, L. Á.; Galindo-de-la-Rosa, J.; Arjona, N.; Guerra-Balcázar, M. 2019 19th International Conference on Micro and Nanotechnology for Power Generation and Energy Conversion Applications (PowerMEMS), IEEE: 2019; pp 1-6.

21. Singh, P.; Mandal, S.; Roy, D.; Chanda, N., *ACS Biomater.Sci. Eng.* 2021, **7** (7), 3446-3458.